Electronic Supplementary Information

For

Synthesis optimization of the ultra-microporous $[Ni_3(HCOO)_6]$ framework to improve its CH_4/N_2 separation selectivity

Xinyu Ren,[a,b] Tianjun Sun,*[a] Jiangliang Hu,[a,b] and Shudong Wang*[a,c]

[a] Dalian National Laboratory for Clean Energy, Dalian Institute of Chemical Physics, Chinese Academy of Sciences, Dalian 116023, P. R. China.

[b] University of Chinese Academy of Sciences, Beijing 100049, P. R. China

[c] State Key Laboratory of Catalysis, Dalian Institute of Chemical Physics, Chinese Academy of Sciences, Dalian 116023, China

Corresponding Authors

* E-mail: wangsd@dicp.ac.cn (Shudong Wang); suntianjun@dicp.ac.cn (Tianjun Sun).

Section S1 Schematic set-up for breakthrough experiments

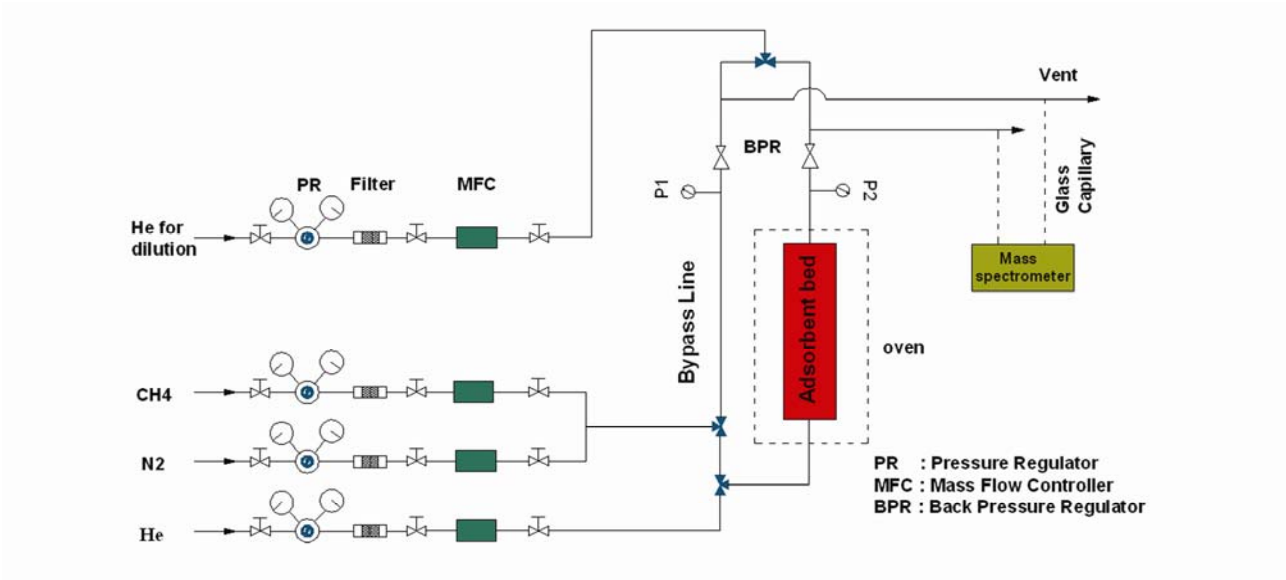

Fig. S1 Apparatus used for collection of breakthrough curves.

Section S2 Thermal stability analysis

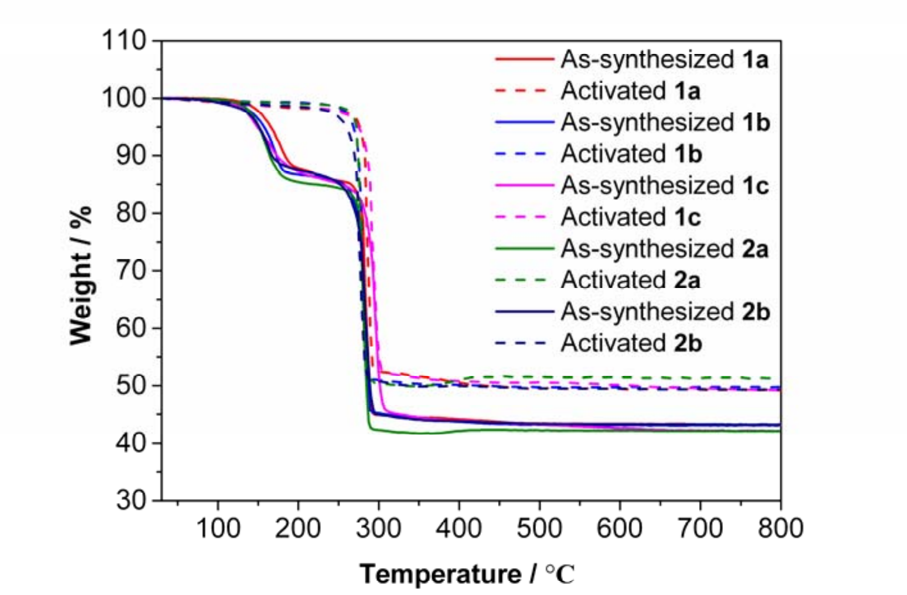

Fig. S2 TGA curves of $[Ni_3(HCOO)_6]$ samples in air atmosphere.

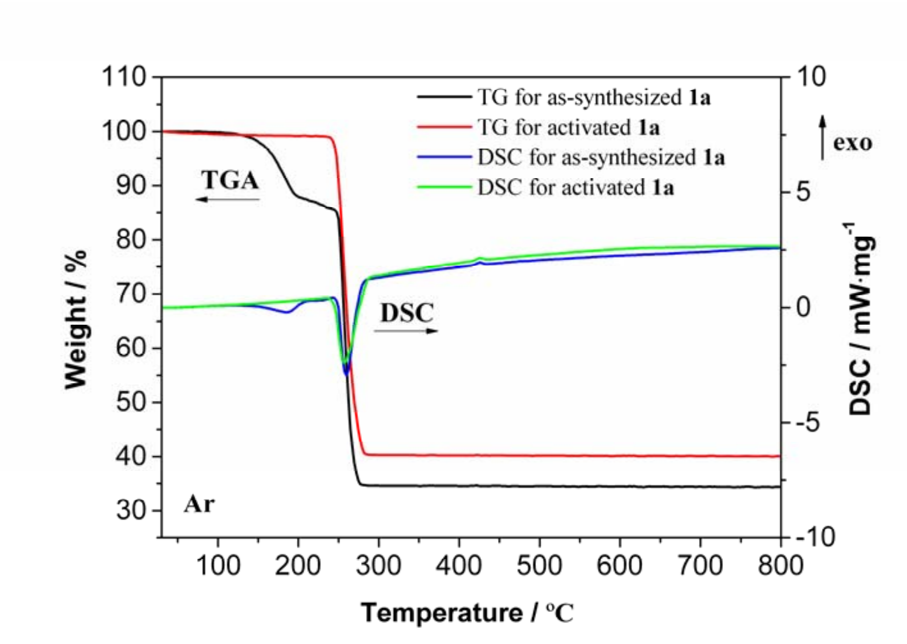

Fig. S3 TGA/DSC curves of Sample **1a** in Ar atmosphere**.**

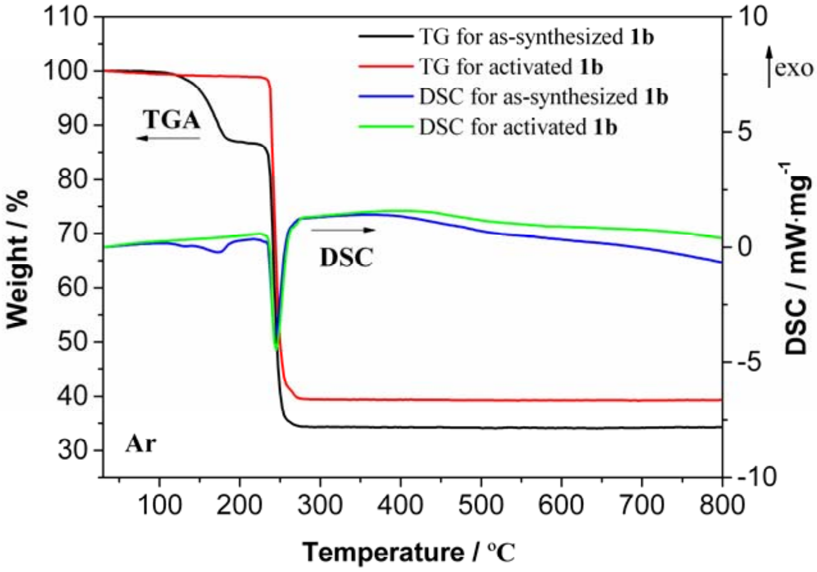

Fig. S4 TGA/DSC curves of Sample **1b** in Ar atmosphere**.**

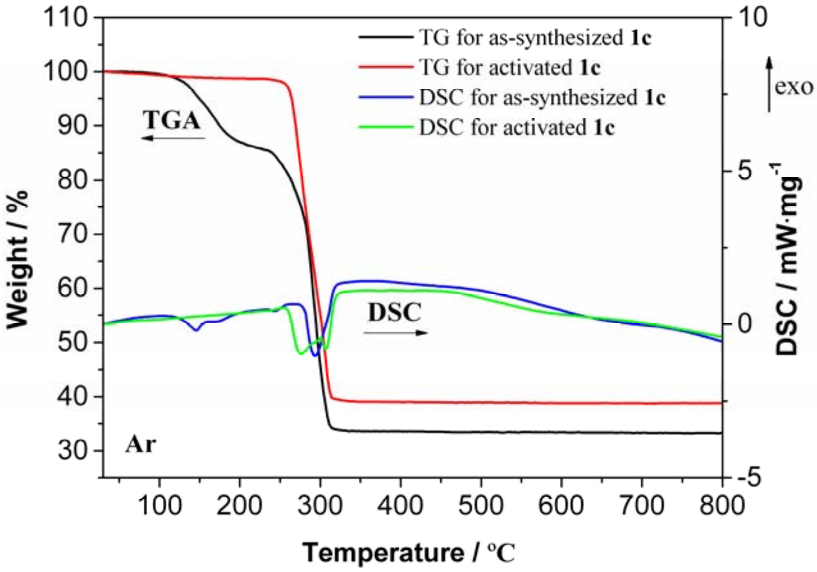

Fig. S5 TGA/DSC curves of Sample **1c** in Ar atmosphere**.**

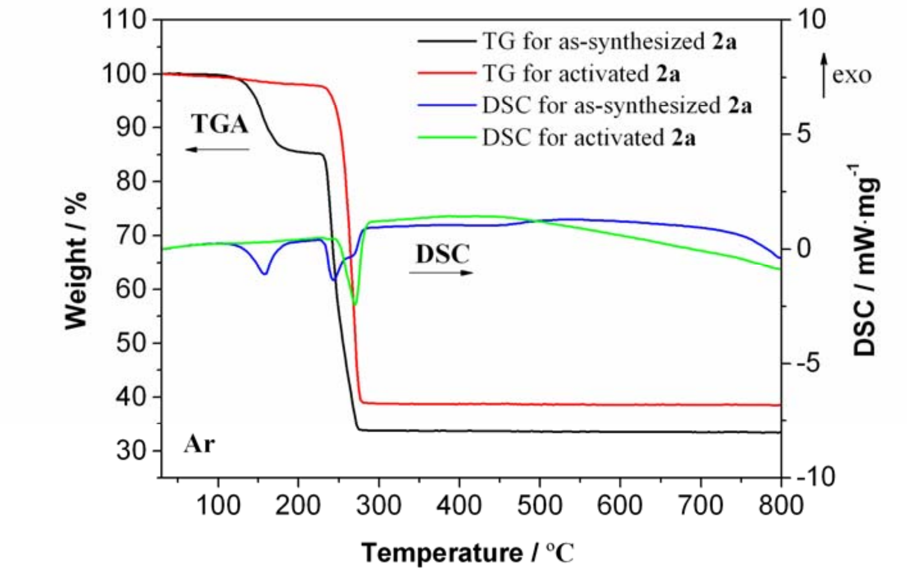

Fig. S6 TGA/DSC curves of Sample **2a** in Ar atmosphere**.**

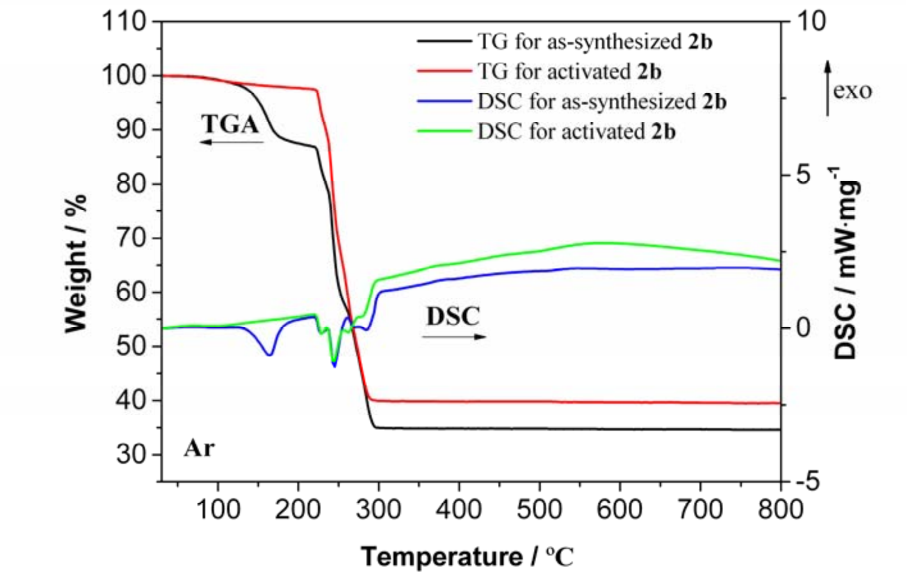

Fig. S7 TGA/DSC curves of Sample **2b** in Ar atmosphere**.**

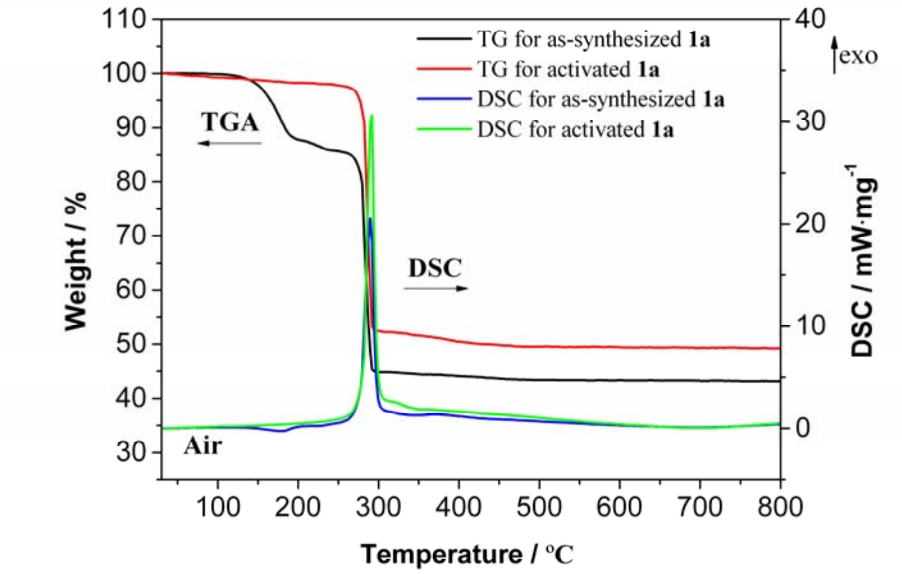

Fig. S8 TGA/DSC curves of Sample **1a** in air atmosphere**.**

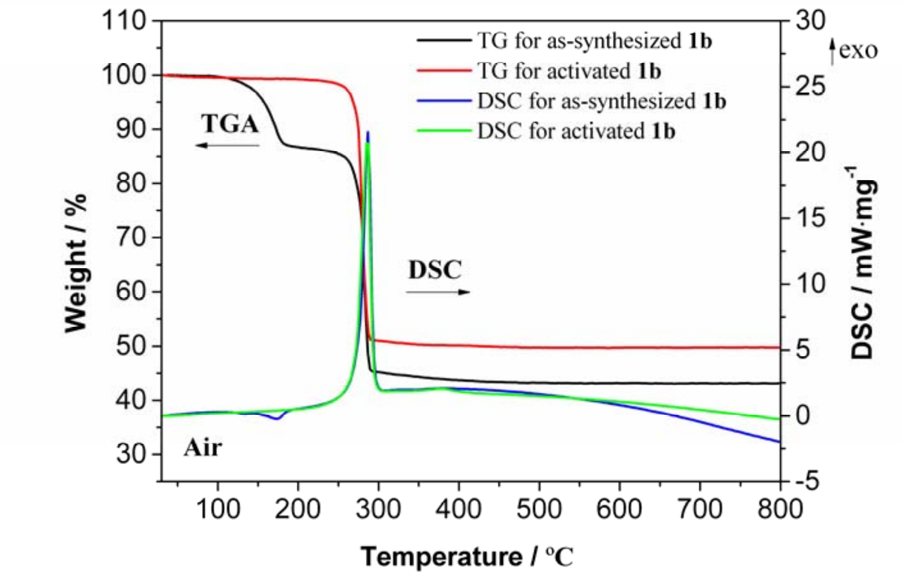

Fig. S9 TGA/DSC curves of Sample **1b** in air atmosphere**.**

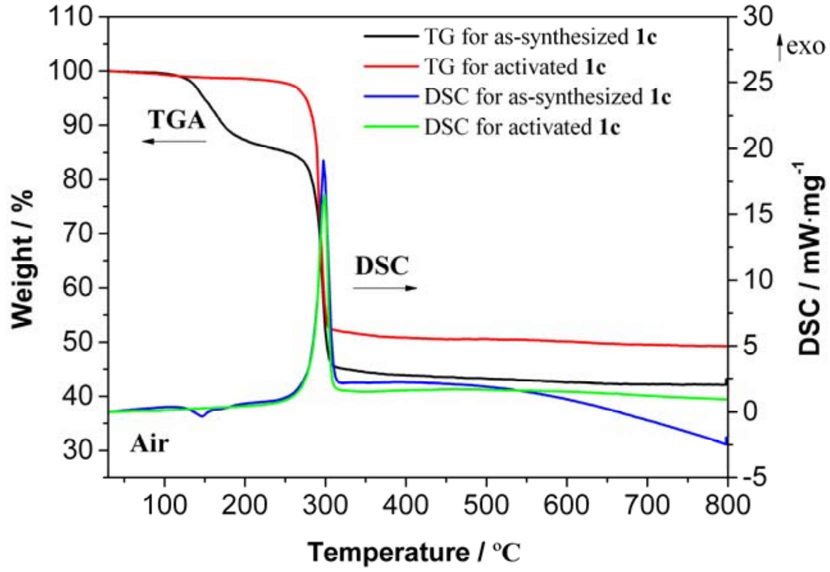

Fig. S10 TGA/DSC curves of Sample **1c** in air atmosphere**.**

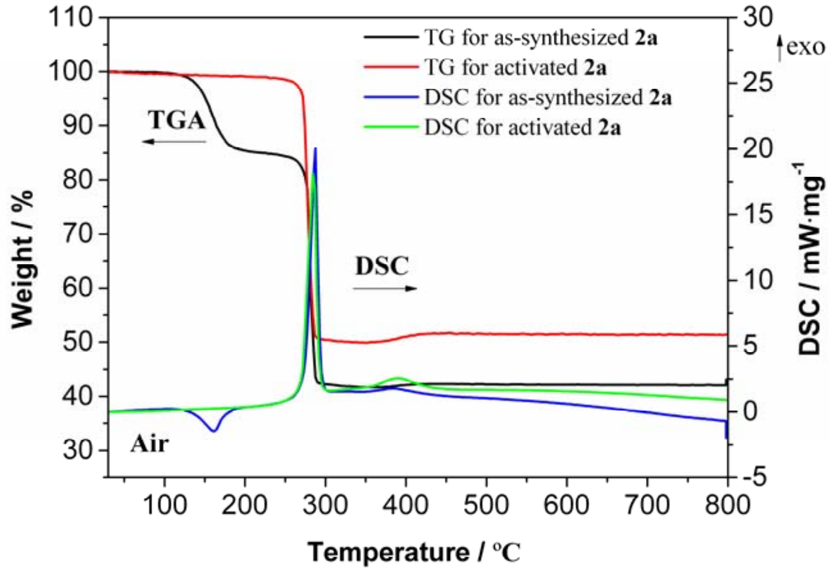

Fig. S11 TGA/DSC curves of Sample **2a** in air atmosphere**.**

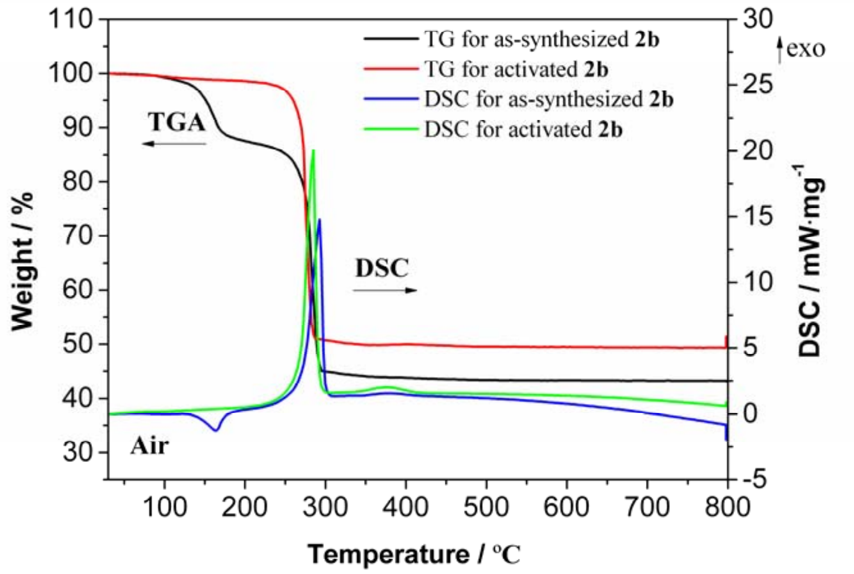

Fig. S12 TGA/DSC curves of Sample **2b** in air atmosphere**.**

Section S3 Chemical stability analysis

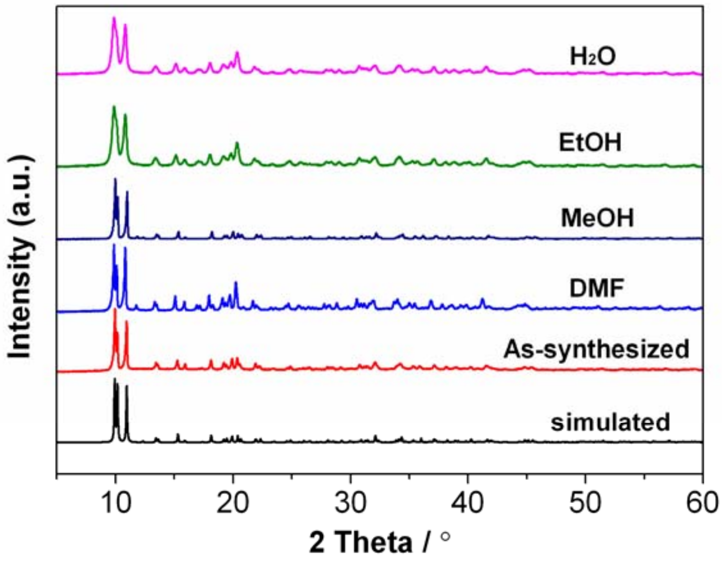

Fig. S13 PXRD patterns of [$Ni_3(HCOO)_6$] samples collected for stability test in DMF, Methanol, Ethanol and water at 100 ºC for 24 hours.

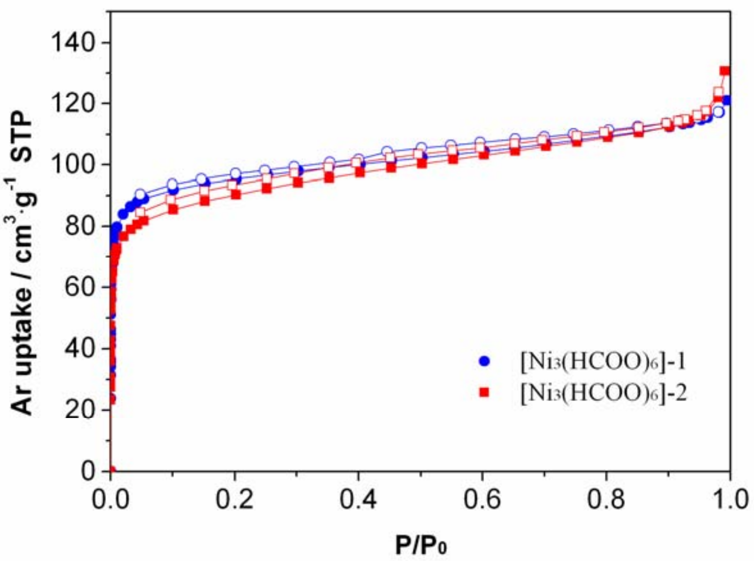

Fig. S14 Ar adsorption isotherms of [$Ni_3(HCOO)_6$]-1 and [$Ni_3(HCOO)_6$]-2 after water treatment.

Section S4 CH_4 and N_2 adsorption data

Table S1

Parameters from low pressure gas adsorption isotherm modelling by Toth model for CH_4 and N_2 adsorption on Sample **1a** at different temperatures and the ideal selectivities at zero coverage calculated from Henry's law constants

Pure gas isotherm model	Parameter/Unit	288 K	298 K	308 K
Toth			**CH_4**	
$N = N_{max} \times B \times P$ /	N_{max}/mmol·g^{-1}	2.196	2.056	1.979
$(1+(B \times P)^c)^{1/c}$	B/torr^{-1}	8.835E-04	6.992E-04	5.247E-04
	c	1.119	1.134	1.154
	K_H/mmol·(g·torr)$^{-1}$	1.940E-03	1.437E-03	1.039E-03
	R^2	0.99999	0.99999	0.99999
	D_n/%	0.001	0.339	0.173
			N_2	
	N_{max}/mmol·g^{-1}	1.829	1.561	1.481
	B/torr^{-1}	1.758E-04	1.514E-04	1.239E-04
	c	1.106	1.156	1.143
	K_H/mmol·(g·torr)$^{-1}$	3.215E-04	2.363E-04	1.835E-04
	R^2	1.00000	1.00000	0.99999
	D_n/%	0.354	0.520	0.812
Ideal selectivity				
$S_{CH_4/N_2} = K_{H,CH_4} / K_{H,N_2}$		6.0	6.1	5.7

Table S2

Parameters from low pressure gas adsorption isotherm modelling by Toth model for CH_4 and N_2 adsorption on Sample **1b** at different temperatures and the ideal selectivities at zero coverage calculated from Henry's law constants

Pure gas isotherm model	Parameter/Unit	288 K	298 K	308 K
Toth			**CH_4**	
$N = N_{max} \times B \times P$ /	N_{max}/mmol·g^{-1}	2.095	2.091	2.075
$(1+(B \times P)^c)^{1/c}$	B/torr^{-1}	9.611E-04	6.822E-04	5.052E-04
	c	1.160	1.173	1.155
	K_H/mmol·(g·torr)$^{-1}$	2.013E-03	1.427E-03	1.048E-03
	R^2	1.00000	1.00000	1.00000
	D_n/%	0.192	0.870	0.435
			N_2	
	N_{max}/mmol·g^{-1}	1.629	1.220	0.832
	B/torr^{-1}	2.026E-04	2.030E-04	2.227E-04
	c	1.184	1.303	1.505
	K_H/mmol·(g·torr)$^{-1}$	3.302E-04	2.476E-04	1.853E-04
	R^2	1.00000	1.00000	1.00000
	D_n/%	0.562	0.988	1.480
Ideal selectivity				
$S_{CH_4/N_2} = K_{H,CH_4} / K_{H,N_2}$		6.1	5.8	5.7

Table S3

Parameters from low pressure gas adsorption isotherm modelling by Toth model for CH_4 and N_2 adsorption on Sample **1c** at different temperatures and the ideal selectivities at zero coverage calculated from Henry's law constants

Pure gas isotherm model	Parameter/Unit	288 K	298 K	308 K
Toth			**CH_4**	
$N = N_{max} \times B \times P$ /	N_{max}/mmol·g^{-1}	1.880	1.858	1.852
$(1+(B \times P)^c)^{1/c}$	B/torr^{-1}	9.527E-04	7.018E-04	5.086E-04
	c	1.142	1.158	1.133
	K_H/mmol·(g·torr)$^{-1}$	1.791E-03	1.304E-03	9.417E-04
	R^2	1.00000	1.00000	1.00000
	D_n/%	0.538	0.344	0.558
			N_2	
	N_{max}/mmol·g^{-1}	1.735	1.116	0.790
	B/torr^{-1}	1.702E-04	1.963E-04	2.050E-04
	c	1.106	1.291	1.458
	K_H/mmol·(g·torr)$^{-1}$	2.953E-04	2.190E-04	1.621E-04
	R^2	1.00000	1.00000	1.00000
	D_n/%	0.716	1.110	1.850
Ideal selectivity				
$S_{CH_4/N_2} = K_{H,CH_4} / K_{H,N_2}$		6.1	6.0	5.8

Table S4

Parameters from low pressure gas adsorption isotherm modelling by Toth model for CH_4 and N_2 adsorption on sample **2a** at different temperatures and the ideal selectivities at zero coverage calculated from Henry's law constants

Pure gas isotherm model	Parameter/Unit	288 K	298 K	308 K
Toth			**CH_4**	
$N = N_{max} \times B \times P$ / $(1+(B \times P)^c)^{1/c}$	N_{max}/mmol·g^{-1}	2.103	2.102	2.101
	B/torr^{-1}	9.78E-04	7.10E-04	5.03E-04
	c	1.156	1.141	1.125
	K_H/mmol·(g·torr)$^{-1}$	2.057E-03	1.492E-03	1.056E-03
	R^2	1.00000	1.00000	1.00000
	D_n/%	0.180	0.266	0.347
			N_2	
	N_{max}/mmol·g^{-1}	0.887	0.393	0.349
	B/torr^{-1}	3.541E-04	5.865E-04	4.884E-04
	c	1.729	2.838	2.968
	K_H/mmol·(g·torr)$^{-1}$	3.140E-04	2.302E-04	1.705E-04
	R^2	0.99999	0.99999	0.99998
	D_n/%	3.912	4.762	7.967
Ideal selectivity				
$S_{CH_4/N_2} = K_{H,CH_4} / K_{H,N_2}$		6.6	6.5	6.2

Table S5

Parameters from low pressure gas adsorption isotherm modelling by Toth model for CH_4 and N_2 adsorption on sample **2b** at different temperatures and the ideal selectivities at zero coverage calculated from Henry's law constants

Pure gas isotherm model	Parameter/Unit	288 K	298 K	308 K
Toth			**CH_4**	
$N = N_{max} \times B \times P$ /	N_{max}/mmol·g^{-1}	1.187	1.149	1.117
$(1+(B \times P)^c)^{1/c}$	B/torr^{-1}	8.869E-04	6.463E-04	4.807E-04
	c	1.122	1.144	1.128
	K_H/mmol·(g·torr)$^{-1}$	1.053E-03	7.427E-04	5.369E-04
	R^2	1.00000	1.00000	1.00000
	D_n/%	0.775	0.700	0.592
			N_2	
	N_{max}/mmol·g^{-1}	0.912	0.546	0.291
	B/torr^{-1}	2.389E-04	2.873E-04	3.851E-04
	c	1.351	1.619	2.148
	K_H/mmol·(g·torr)$^{-1}$	2.180E-04	1.570E-04	1.119E-04
	R^2	0.99999	0.99999	0.99998
	D_n/%	3.425	2.722	5.047
Ideal selectivity				
$S_{CH_4/N_2} = K_{H,CH_4} / K_{H,N_2}$		4.8	4.7	4.8

Section S5 Breakthrough separation experiments

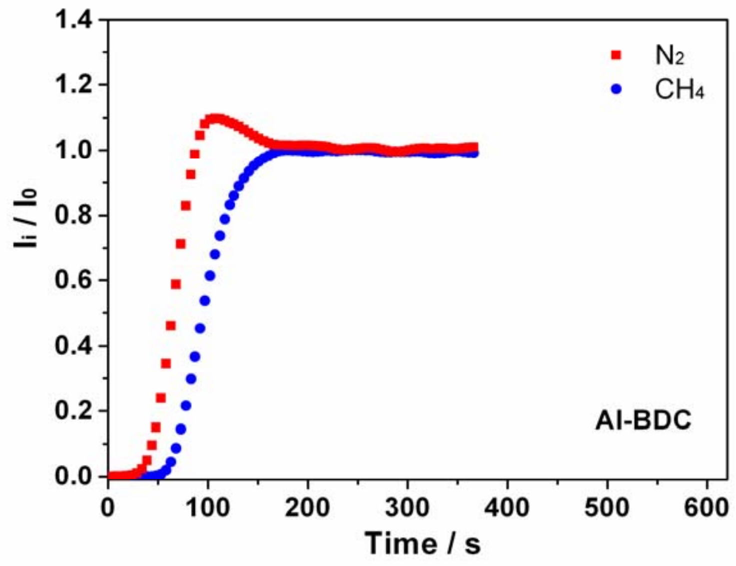

Fig. S15 Breakthrough curves of the CH_4-N_2 equimolar mixture at 298 K and 2.0 bar on Al-BDC.

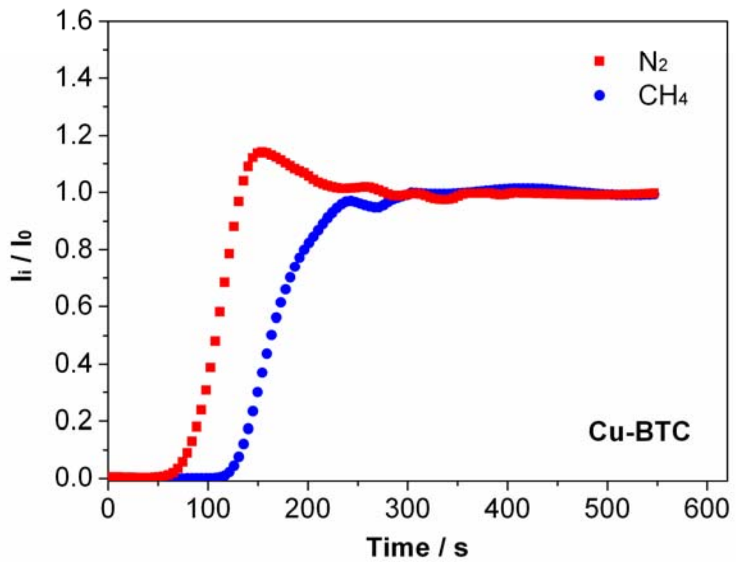

Fig. S16 Breakthrough curves of the CH_4-N_2 equimolar mixture at 298 K and 2.0 bar on Cu-BTC.

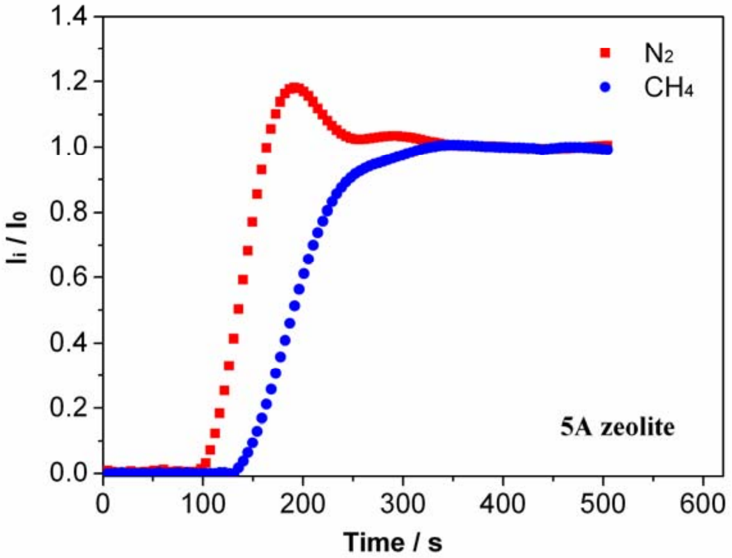

Fig. S17 Breakthrough curves of the CH_4-N_2 equimolar mixture at 298 K and 2.0 bar on 5A zeolite.

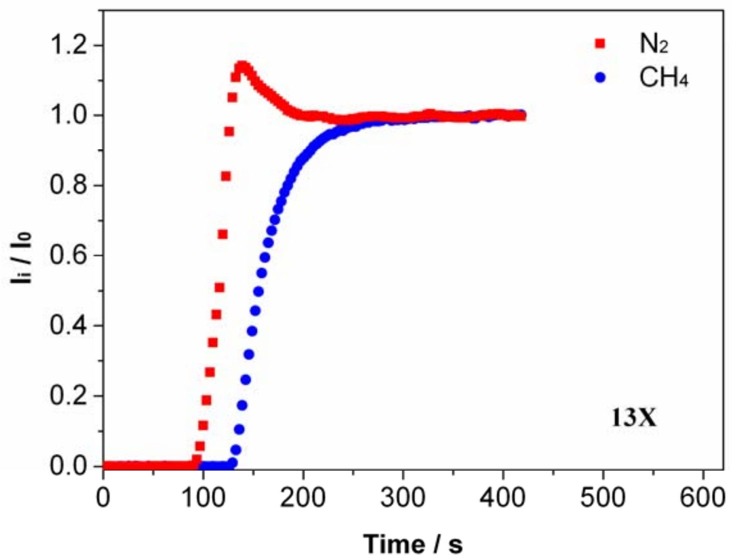

Fig. S18 Breakthrough curves of the CH_4-N_2 equimolar mixture at 298 K and 2.0 bar on 13X zeolite.

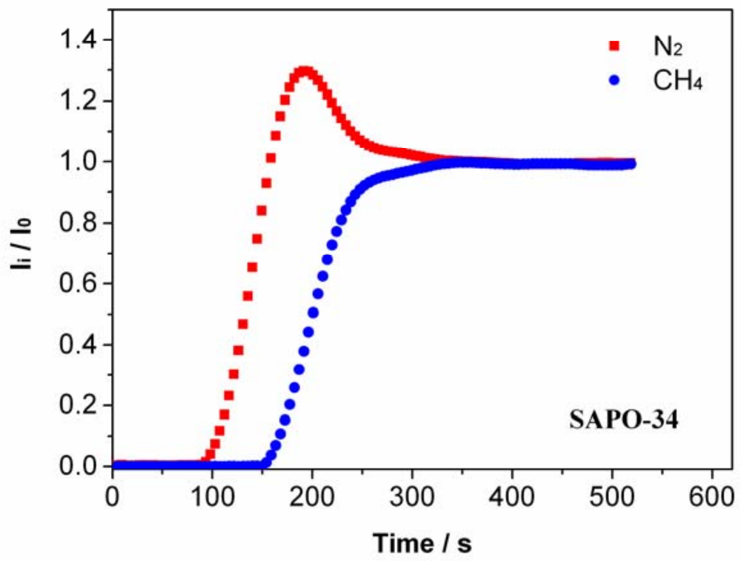

Fig. S18 Breakthrough curves of the CH_4-N_2 equimolar mixture at 298 K and 2.0 bar on SAPO-34.

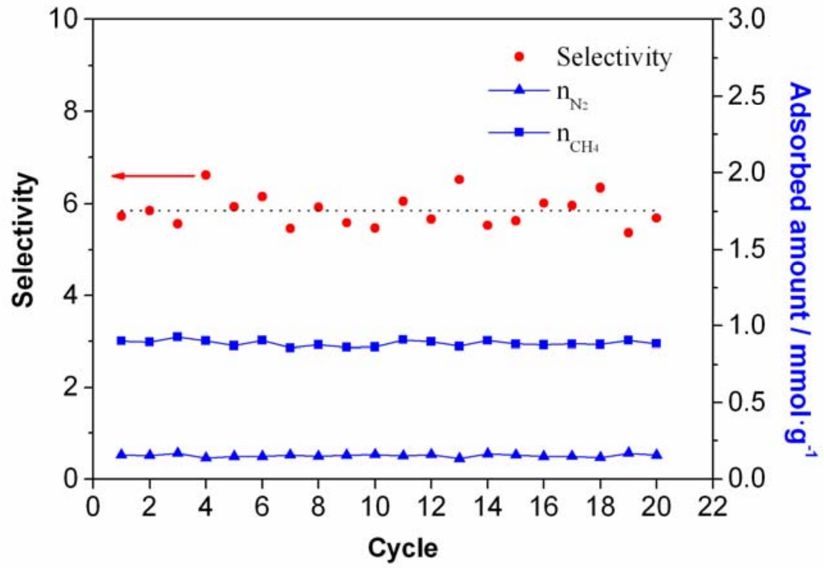

Fig. S19 Stability of regeneration for Sample **1a**.